



Mono and binary component biosorption of Cu(II), Ni(II), and Methylene Blue onto raw and pretreated *S. cerevisiae*: equilibrium and kinetics

Ulker Asli Guler*, Meltem Sarioglu

Engineering Faculty, Department of Environmental Engineering, Cumhuriyet University, Sivas 58140, Turkey
Tel. +90 346 219 10 10 1295; Fax: +90 346 219 11 77; email: ulkerasli@gmail.com

Received 10 May 2012; Accepted 9 May 2013

ABSTRACT

The mono and binary biosorption of Cu(II) ions, Ni(II) ions, and Methylene Blue dye onto raw and pretreated *S. cerevisiae* was investigated in a batch system. The biosorption mechanism was characterized by FT-IR, XRD, and SEM analyses. The effects of pH, contact time, initial pollutant concentration, temperature, and biosorbent dosage on the biosorption studies were determined. The experimental data were analyzed by Langmuir, Freundlich, and Dubinin–Radushkevich isotherm models. The results were compatible with both Langmuir and Freundlich isotherm models. The mean free energy (E) values indicated that the biosorption of Cu(II), Ni(II), and Methylene Blue onto raw and pretreated *S. cerevisiae* took place by chemical-ion exchange. Kinetic data fitted well into the pseudo-second-order model. The calculated thermodynamic parameters (ΔH , ΔS , and ΔG) showed that the biosorption of Cu(II), Ni(II), and Methylene Blue onto raw and pretreated *S. cerevisiae* was exothermic and spontaneous. Desorption, ion selectivity, and the effect of ionic strength (NaCl) studies were also conducted. Competitive biosorption of binary mixtures of Cu(II), Ni(II), and MB was investigated in terms of biosorption capacity and found that the biosorption capacity of biosorbent decreased with increasing competing pollutant concentration.

Keywords: Biosorption; Yeast (*S. cerevisiae*); Pretreated; Methylene Blue; Heavy metal

1. Introduction

Heavy metal and dye pollution in industrial areas is one of the most important environmental problems. These pollutants are discharged from different industries such as textile, mining, electroplating, leather, dyehouse, ceramic, and glass industries into aquatic ecosystems [1–3]. Heavy metals are extremely dangerous for human life and environmental health due to their toxicity and accumulation in the food chain.

Dyes also negatively affect the photosynthetic activity by reducing light penetration in aquatic ecosystem [3–6]. Conventional treatment methods such as electrochemical treatment, ion exchange, chemical precipitation, chemical oxidation, membrane technologies, evaporation recovery, reverse osmosis, and coagulation–flocculation are used for the removal of heavy metal and dyes from wastewaters [3,6,7]. These processes have disadvantages such as low effectiveness, high cost, and production of excessive toxic sludge.

*Corresponding author.

Therefore, new treatment processes for the removal of heavy metal and dyes from wastewaters are needed [5,8,9]. Biosorption has been developed as an alternative treatment method for the removal of these types of pollutants. Biosorption is defined as the removal of heavy metal and dyes from wastewaters through biomaterials such as bacteria, fungi, yeasts, and algae etc. It is a simple, efficient, and inexpensive process. The heavy metal and dyes in wastewaters are biosorbed on the cell surface by interaction with the chemical functional groups such as carboxylate, amine, amide, phosphate, sulfide, and other functional groups found on the cell walls of biomaterials [6,10,11]. The advantages of biomaterials are the diversity of active binding areas, small and uniform structure, and high metal-binding capacity [3,10,12]. *S. cerevisiae* yeast is widely used as biosorbent among these favorable biomaterials for heavy metal removal. It can be easily grown using simple fermentation techniques, its growth media is inexpensive, it can be obtained from various food and beverage industry, and it is not pathogenic. In addition, *S. cerevisiae* yeast is an ideal organism model for the determination of biosorption mechanism [9,13]. Therefore, in this study, *S. cerevisiae* yeast is preferred as biosorbent.

The objective of this study is to investigate the comparison of mono and binary component biosorption of Cu(II), Ni(II) ions, and Methylene Blue dye from aqueous solutions by using raw and detergent-pretreated *S. cerevisiae*, because some real industrial wastewaters contain mixture of metal and dyes. There are some studies on the mono component biosorption. However, the studies dealing with binary component biosorption are limited [14,15].

In this study, the surface structure and surface functional groups of the biosorbent were characterized through SEM, XRD, and FT-IR analyses, respectively. The parameters related to biosorption such as initial solution pH, contact time, initial pollutant concentration, temperature, biosorbent dosage, ionic strength, and ionic selectivity were optimized. The equilibrium data were evaluated by Langmuir, Freundlich, and Dubinin–Radushkevich (D–R) isotherm models. Kinetic parameters were calculated by using pseudo-first-order kinetic model, pseudo-second-order kinetic model, and intraparticle diffusion model. The effectiveness of different desorbents (NaOH, HCl, and laundry detergent) to remove the biosorbed metal and dye from the biosorbent was also investigated. In addition, competitive biosorptions of binary mixtures (Cu(II)–Ni(II) and Cu(II)–MB) onto raw and pretreated *S. cerevisiae* were investigated and compared with the mono component systems.

2. Material and methods

2.1. Biosorbent

S. cerevisiae was provided as waste granule yeast from Turkey–İzmir Pakmaya Factory. Before use, the yeast was washed with distilled water and dried at 60°C in oven. Specific surface areas of raw and pretreated *S. cerevisiae* were found to be 9.62 m²/g and 6.99 m²/g by BET analysis, respectively.

2.2. Pretreatment of *S. cerevisiae*

An amount of *S. cerevisiae* yeast (25 g wet weight for each procedure) was subjected to pretreatment with different procedures including chemical and physical methods in order to increase its biosorption capacity: (a) pretreatment with alkali solution (0.1 M NaOH (sodium hydroxide), commercial laundry detergent (30 g) (200 mL)); (b) pretreatment with acidic solutions (10% CH₂O (formaldehyde), 10% CH₃COOH (acetic acid), 10% C₂H₅OH (ethanol) (200 mL)), (c) pretreatment with salt solutions (0.1 M NaCl (sodium chloride), 0.1 M CaCl₂ (calcium chloride) (200 mL)) in a shaker at 130 rpm for 24 h, and (d) *S. cerevisiae* was autoclaved for 30 min at 1 bar pressure at 121°C [16]. The biosorbent was washed with distilled water after each pretreatment procedure until a neutral pH (7.0 ± 0.2) is reached and then dried at 60°C in oven.

2.3. Biosorption experiments

Biosorption experiments were conducted in Erlenmeyer with 100 mL of aqueous solutions. The pH was adjusted with HCl and NaOH. The suspension was shaken in a temperature-controlled shaker at 120 rpm. The suspension was then centrifuged for 5 min at 4,000 rpm and the heavy metal ions (Cu(II) and Ni(II)) in the supernatant were measured using an atomic absorption spectrometer (GBC Avanta Σ) at 217.9 and 351.5 nm wavelengths, respectively. MB in the supernatant was analyzed by CHEBIOUS UV-spectrophotometer at 663 nm wavelength. In addition, it was determined that λ_{max} value (663 nm) of MB dye was not affected by pH, which was established by λ_{max} scanning at different pH values. The chemical structure of MB cationic dye (C₁₆H₁₈N₃SCl.3H₂O) is given in Fig. 1 [1].

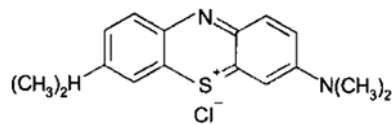


Fig. 1. The chemical structure of Methylene Blue dye.

The details of the experimental conditions for mono component biosorption are presented in Table 1.

The biosorption capacity (q_e , mg/g) and removal efficiency (%) were determined using the following equations:

$$q_e = \frac{(C_o - C_e)V}{m} \tag{1}$$

$$\text{Removal efficiency (\%)} = \frac{C_o - C_e}{C_o} \times 100 \tag{2}$$

where C_o and C_e are the initial and the equilibrium pollutant concentrations (mg/L), V is the volume of solution (L), and m is the amount of biosorbent (g).

The difference between the biosorption capacity of raw and pretreated biosorbent was calculated by using the following equation [17]:

$$\Delta q_e = \frac{q_{e,2} - q_{e,1}}{q_{e,1}} \times 100 \tag{3}$$

where $q_{e,2}$ and $q_{e,1}$ are the amounts of pollutants biosorbed on the pretreated and raw biosorbent at equilibrium (mg/g), respectively.

2.4. Isotherm models

All isotherm models parameters were calculated by non-linear regression by using SigmaPlot 8 software. The Langmuir isotherm essentially describes the monolayer type of adsorption.

It is expressed as follows [18]:

$$q_e = \frac{Q_m b C_e}{1 + b C_e} \tag{4}$$

where Q_m (mg/g) is the maximum adsorption capacity and b (L/mg) is the Langmuir constant

related to the affinity between sorbent and sorbate. The essential feature of the Langmuir isotherm can be expressed in terms of R_L , a dimensionless constant referred to as separation factor or equilibrium parameter. R_L is calculated using the following equation [18,19]:

$$R_L = \frac{1}{1 + b C_o} \tag{5}$$

The value of R_L indicates the type of the isotherm to be irreversible ($R_L=0$), favorable ($0 < R_L < 1$), linear ($R_L=1$), or unfavorable ($R_L > 1$).

The Freundlich isotherm is derived to model multilayer adsorption and adsorption on heterogeneous surfaces. The Freundlich isotherm is given by the equation [20]:

$$q_e = k_F C_e^{\frac{1}{n}} \tag{6}$$

where k_F (L/g) is the Freundlich adsorption constant related to the adsorption capacity and n is the adsorption intensity. The $1/n$ value was between 0 and 1, indicating that the adsorption was favorable at studied conditions [21].

D-R isotherm is more general than the Langmuir isotherm. It was applied to separate the nature of adsorption processes as physical or chemical. The D-R isotherm equation is expressed as follows [22]:

$$q_e = q_{D-R} e^{\beta \varepsilon^2} \tag{7}$$

where q_e (mol/g) is the amount pollutants biosorbed on the biosorbent at equilibrium, q_{D-R} (mol/g) is the maximum adsorption capacity, β (mol²/J²) is a coefficient related to the mean free energy of adsorption, and ε (J/mol) is the Polanyi potential that can be written as:

Table 1
Experimental conditions for mono component biosorption

Set	Aim of experiment	Solution pH	Poll. conc. (mg/L)	Biosorbent dosage (g/L)	Contact time (min)	Temperature
Experimental conditions						
1	Effect of initial solution pH	2–7	100	10	1,440	Room temperature (20 °C)
2	Effect of initial pollutant concentration	Opt. pH	25–300	10	1,440	Room temperature (20 °C)
3	Effect of biosorbent dosage	Opt. pH	Opt. init. con.	1–10	1,440	Room temperature (20 °C)
4	Effect of contact time	Opt. pH	Opt. init. con.	Opt. dosage	5–1,440	Room temperature (20 °C)
6	Effect of temperature	Opt. pH	Opt. init. con.	Opt. dosage	Opt. cont. time	20–50 °C
7	Effect of ionic strength (0.01–1.00 M NaCl)	Opt. pH	Opt. init. con.	Opt. dosage	Opt. cont. time	Room temperature (20 °C)

$$\varepsilon = RT \ln \left(1 + \frac{1}{C_e} \right) \quad (8)$$

The constant β gives an idea about the mean free energy E (kJ/mol) of adsorption, which can be calculated using the relationship:

$$E = \frac{1}{\sqrt{-2\beta}} \quad (9)$$

If E value is between 8 and 16 kJ/mol, the adsorption process follows by chemical ion-exchange and if $E < 8$ kJ/mol, the adsorption process is likely physical adsorption [23,24].

2.5. Kinetic modeling

Kinetic models such as Lagergen pseudo-first-order model, Ho's pseudo-second-order model, and intraparticle diffusion model in order to investigate the rate controlling mechanism of adsorption process have been applied to experimental data [5,6,18,25].

The Lagergen pseudo-first-order kinetic model is given as:

$$\log(q_e - q_t) = \log q_e - \frac{k_1}{2.303}t \quad (10)$$

where q_t (mg/g) is the amount of adsorbed pollutant on the adsorbent at time t and k_1 (L/min) is the rate constant of pseudo-first-order kinetic model. A straight line of $\log(q_e - q_t)$ vs. t suggests the applicability of this kinetic model. q_e and k_1 can be determined from the intercept and slope of the plot, respectively.

The pseudo-second-order kinetic model is expressed as:

$$\frac{t}{q_t} = \frac{1}{k_2(q_e)^2} + \frac{t}{q_e} \quad (11)$$

where k_2 (g/mg.min) is the rate constant of pseudo-second-order kinetic model. The plot t/q_t vs. t should give a straight line if second order kinetics is applicable and q_e and k_2 can be determined from the slope and intercept of the plot, respectively [18,25].

The intraparticle diffusion model equation can be calculated in the following way [26]:

$$q_t = k_d t^{0.5} + C \quad (12)$$

where C is the intercept and k_d is the intraparticle diffusion rate constant (mg/gmin^{0.5}), which can be eval-

uated from the slope of the linear plot of q_t vs. $t^{0.5}$. q_t is the amount of sorbate on the surface of the biosorbent at time t (mg/g), and t is the time (min). According to this model, the plot of q_t vs. $t^{0.5}$ should be linear ($C=0$) if intraparticle diffusion is involved in the overall biosorption mechanism. Furthermore, if this line passes through the origin, then the intraparticle diffusion is the sole rate-controlling step of the process.

The following expression denotes the initial adsorption rate h (mg/g min):

$$h = k_2 q_e^2 \quad (13)$$

where h (mg/g min) is the initial adsorption rate.

2.6. Evaluation of thermodynamic parameters

Thermodynamic parameters such as energy and entropy factors were considered in order to determine whether adsorption occurred spontaneously or not [5]. These thermodynamic parameters of the adsorption reaction are given by the following equations [11,21,27,28]:

$$\Delta G = -RT \ln K_C \quad (14)$$

where ΔG is the Gibbs free energy change, R is the universal gas constant (8.314 J/mol K), T is the temperature (K), and K_C (q_e/C_e) is the equilibrium constant.

The enthalpy change (ΔH) and entropy change (ΔS) parameters were estimated from the following equation:

$$\ln K_C = \frac{\Delta S}{R} - \frac{\Delta H}{RT} \quad (15)$$

where ΔH and ΔS in the biosorption process were determined from a slope and intercept of the plot of $\ln K_C$ vs. $1/T$, respectively. The value of ΔH and ΔG were negative, indicating that the adsorption process is exothermic and spontaneous. The positive value of ΔS shows the increase in randomness at the solid/liquid interface during the adsorption process [29].

3. Results and discussion

3.1. Pretreatment

The effect of pretreatment on the biosorption of Cu (II), Ni(II), and MB onto *S. cerevisiae* is given in Table 2. The results indicate that the pretreatment of *S. cerevisiae* with laundry detergent enhanced the biosorption

Table 2

The effect of pretreatment on the biosorption of Cu(II), Ni(II), and MB onto *S. cerevisiae*

Pretreatment methods									
Raw biosorbent	Acidic solutions			Alkali solutions		Salt solutions		Physical methods	
	Acetic acid (10%)	Formaldehyde (10%)	Ethanol (10%)	0.1 M NaOH	Laundry detergent	0.1 M CaCl ₂	0.1 M NaCl	Autoclave	
Cu(II)									
q_e (mg/g)	3.61	0.90	3.00	0.19	2.87	4.66	1.75	1.36	3.48
Δq_e (%)	-75.00	-17.00	-95.00	-21.00	29.00	-52.00	-62.00	-4.00	
Ni(II)									
q_e (mg/g)	6.63	3.76	4.14	4.11	4.72	7.57	4.42	4.41	1.45
Δq_e (%)	-43.00	-38.00	-38.00	-29.00	14.00	-33.00	-34.00	-78	
MB									
q_e (mg/g)	9.22	9.35	9.33	9.34	9.26	9.37	9.23	9.32	9.36
Δq_e (%)		1.00	1.00	1.00	0.00	2.00	0.00	1.00	2.00

capacity of raw *S. cerevisiae* for Cu(II), Ni(II), and MB. The Δq_e (%) values for pretreated with laundry detergent were found to be 29, 14, and 2% for Cu(II), Ni(II), and MB, respectively. The pretreatments with alkali solutions such as laundry detergent and sodium hydroxide may cause chemical modification of cell wall components and destruction of autolytic enzymes on the surface of the cell wall leading to the emergence of masked metal-binding sites on the cell wall. In addition, the remaining alkalinity can cause hydrolysis reactions. The hydrolysis reactions can lead to the formation of more carboxylic (-COOH), carboxylate (-COO), and alcohol (-OH) groups in the biosorbent, which increased the cationic biosorption [30–34]. Various researchers reported that the alkali pretreatments of biosorbent increased the biosorption capacity when compared with raw biosorbent [16,17,30,31].

The pretreatment of *S. cerevisiae* with acidic solutions such as acetic acid, formaldehyde, and ethanol decreased the biosorption capacity of *S. cerevisiae* for Cu(II) and Ni(II) ions. This behavior can be referred to the fact that hydrogen ions may bind to the negatively charged surfaces of the biosorbent. This effect is expected to reduce the available active sites for binding the metal ions [35–37].

According to the above results, in this study, *S. cerevisiae* was used as a raw and detergent-pretreated biosorbent.

3.2. Characterization of biosorbent

The FT-IR spectroscopy of raw and detergent-pretreated *S. cerevisiae* was analyzed in order to determine the effect of pretreatment with laundry detergent on the vibrational characteristics of the

functional groups in the biosorbent [2,38,39]. The results are given in Fig. 2.

The spectrum of raw *S. cerevisiae* is very complex due to various functional groups. The fundamental organic functional groups such as carboxyl, amino/hydroxyl, phosphoryl, etc. are located on the cell wall of *S. cerevisiae* [40].

The basic peaks for the functional groups of raw and pretreated *S. cerevisiae* before and after biosorption of Cu(II), Ni(II), and MB are listed in Table 3 [2,39,41,42]. Absorbance peaks were observed in 3,220–3,406, 2,925, 1,649, 1,543, 1,457, 1,398, 1,242, and 1,045 cm⁻¹ bands in the spectrum of raw *S. cerevisiae* (Fig. 2(a)). A decrease in the 3,220–3,406 cm⁻¹ band for raw *S. cerevisiae* loaded with Cu(II) occurred due to the participation between Cu(II) and -NH/-OH [40]. There are changes in the 822, 1,252, 1,464, 2,879, and 2,931 cm⁻¹ bands. These absorption peaks observed in the spectrum indicating amide II, amide III, and carbonyl groups also displayed some modifications. All of these modifications indicate that some portion of the CONH-/COO- groups and Cu(II) formed coordination bonds [43]. There are several functional groups on the cell wall of the *S. cerevisiae* for binding of Ni(II) ions. The FT-IR spectrums of raw *S. cerevisiae*-loaded Ni(II) indicates active functional groups of O-H stretching (3,600–3,200 cm⁻¹), alkane C-H stretching (2,850–2,956 cm⁻¹), -N=O stretching (1,500–1,600 cm⁻¹), amine bending (1,450 cm⁻¹–1,550 cm⁻¹), -N=O stretching (1,400–1,300 cm⁻¹), -C=O stretching (1,625–1,730 cm⁻¹), C-O stretching (1,300–1,000 cm⁻¹), and carboxylic acid (1,000–1,260 cm⁻¹) vibrations. All these data show that the mechanism of the Ni(II) biosorption occurs in the hydroxyl (-O-H), amine (-NH), and carboxylate (-COO-) ion groups of the

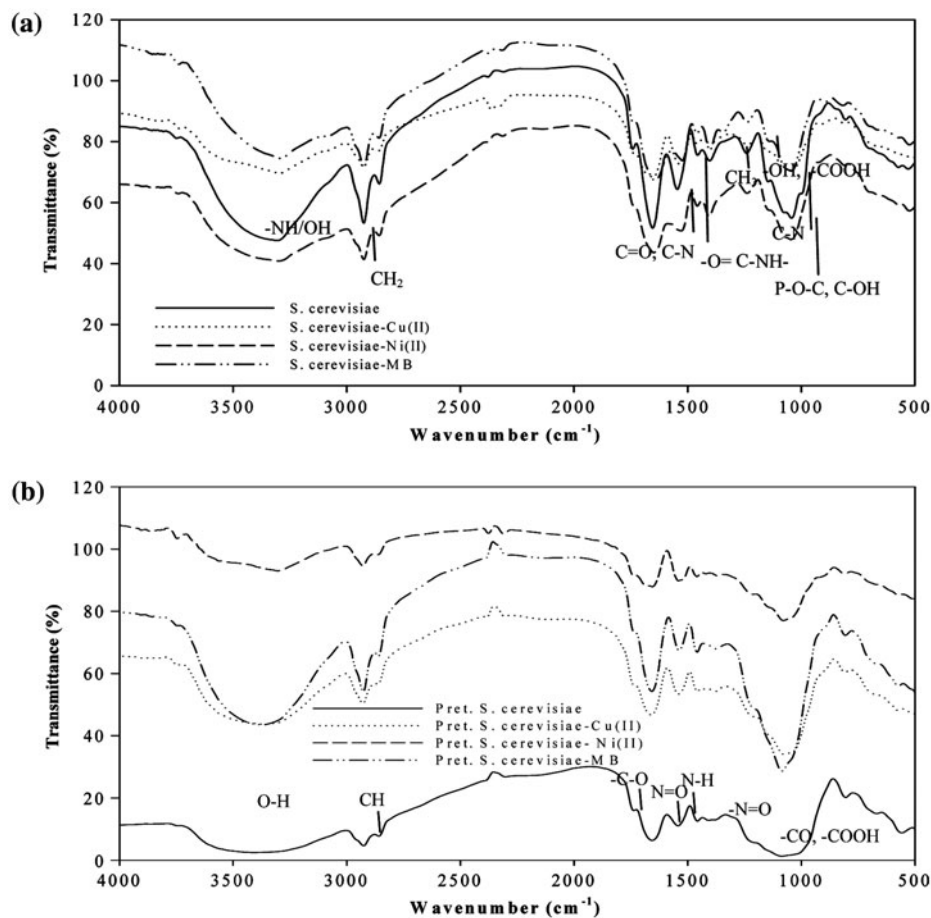


Fig. 2. FT-IR spectra of raw *S. cerevisiae* (a) and laundry detergent-pretreated *S. cerevisiae* (b).

Table 3
FT-IR peaks for raw and pretreated *S. cerevisiae*

FT-IR peak range (cm ⁻¹)	Functional group reported corresponding to the observed peak behavior for raw <i>S. cerevisiae</i>
3,220–3,406	–NH/–OH stretching vibration
2,925	Asymmetric CH ₂ stretching vibration and symmetrical CH ₂ stretching vibration
1,649	C=O, C–N (amide I) stretching vibration
1,543	–O=C–NH– (amide II) bending vibration
1,457	CH ₃ Asymmetric bending vibration and CH ₂ bending vibration
1,398	–OH and –COOH symmetrical vibration
1,242	C–N stretching vibration
1,045	P–O–C and C–OH stretching vibration
FT-IR peak range (cm ⁻¹)	Functional group reported corresponding to the observed peak behavior for <i>S. cerevisiae</i>
3,600–3,200	O–H stretching vibration
2,850–2,956	Alkanes CH stretching vibration
1,730–1,625	–C–O stretching vibration
1,600–1,500	N=O stretching vibration
1,550–1,450	N–H bending vibration
1,400–1,300	–N=O stretching vibration
1,260–1,000	–CO stretching vibration, carboxylic acid
1,300–1,000	–C–O stretching vibration

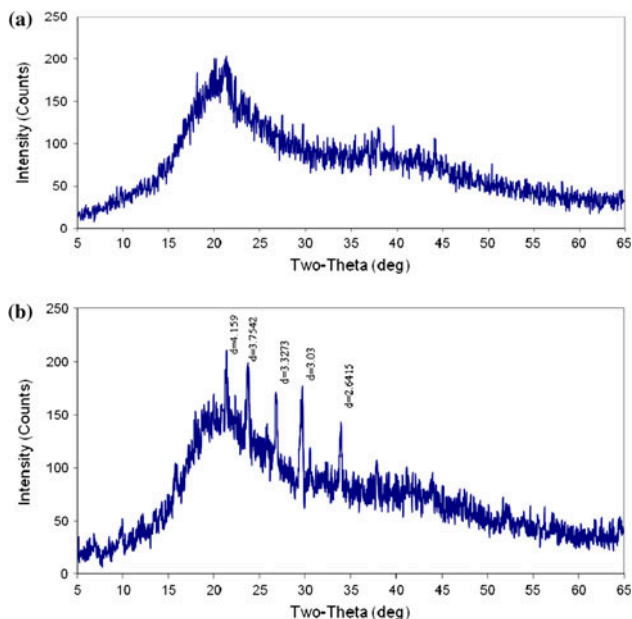


Fig. 3. XRD patterns of raw *S. cerevisiae* (a) and laundry detergent-pretreated *S. cerevisiae* (b).

polysaccharides on the peptidoglycan layer for the metal–biomass interaction on the cell surface [39].

The changes in some peaks observed in the spectrum of pretreated *S. cerevisiae* are a result of the effect of pretreatment with detergent [17]. The decrease in the peaks of 3,600–3,200, 1,600–1,500, and 1,550–1,450 cm^{-1} bands and the increase in the peaks of 1,260–1,000 cm^{-1} bands of pretreated *S. cerevisiae* loaded with Cu, Ni, and MB occurred. These peak deformations observed in the FT-IR spectrum can be evaluated as evidence of biosorption.

The structural transformation and the morphological change of raw and pretreated *S. cerevisiae* have been determined by XRD analyses (Fig. 3(a) and (b)). According to XRD results, the *S. cerevisiae* has amorphous phase.

The SEM images showing the surface structure of raw and pretreated *S. cerevisiae* are given in Figs. 4 and 5. SEM images of raw *S. cerevisiae* (Fig. 4(a)) show spheroidal or slightly elongated spheroidal shapes, and regular and smooth surfaces. The regular surface area is advantageous for biosorption process. According to SEM images of pretreated *S. cerevisiae*, the *S. cerevisiae* surface is covered with detergent (Fig. 5(a)). The shape of raw and pretreated *S. cerevisiae* loaded with Cu(II), Ni(II), and MB did not change much. Cu(II), Ni(II), and MB distributed as spot-like

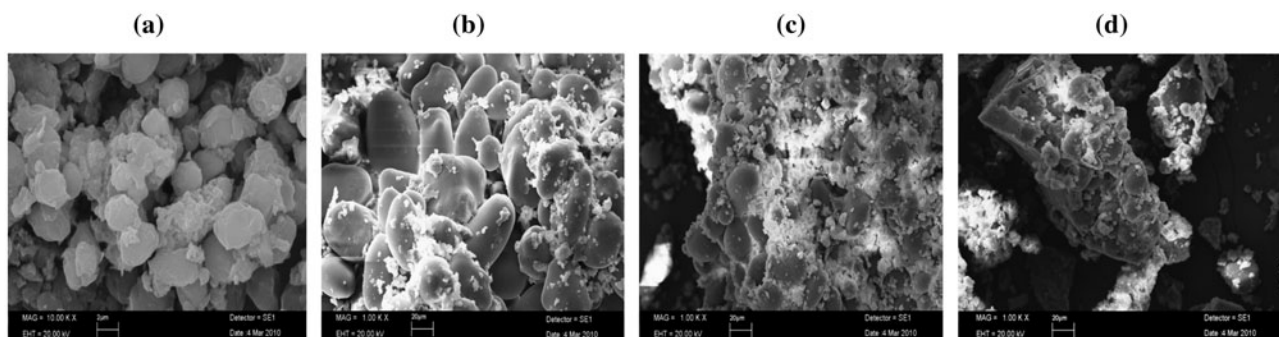


Fig. 4. SEM images; (a) raw *S. cerevisiae*, (b) raw *S. cerevisiae*–Cu(II), (c) raw *S. cerevisiae*–Ni(II), and (d) raw *S. cerevisiae*–MB.

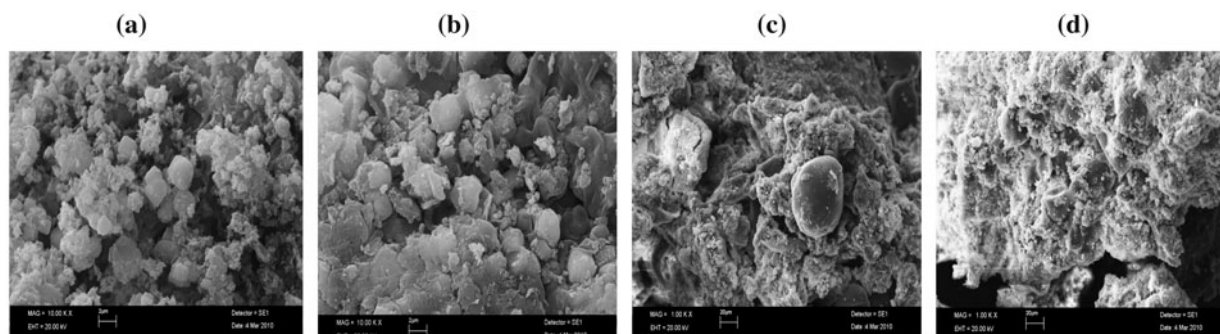


Fig. 5. SEM images; (a) pretreated *S. cerevisiae*, (b) pretreated *S. cerevisiae*–Cu(II), (c) pretreated *S. cerevisiae*–Ni(II), and (d) pretreated *S. cerevisiae*–MB.

particles on the surface of the *S. cerevisiae* cells. These results indicate that the cell wall of the *S. cerevisiae* has played an important role in the biosorption process [2,44,45].

3.3. Effect of solution pH on biosorption

The pH values of solutions are an important environmental factor in the site dissociation of biosorbent surfaces and the solution chemistry of the heavy metals such as hydrolysis, complexation by organic and/or inorganic ligands, redox reactions, precipitation, and biosorption availability of heavy metals [9,46–49]. The effect of pH on the biosorption of Cu(II), Ni(II), and MB is given in Fig. 6(a) and (b).

The results show that the biosorption capacity for Cu(II), Ni(II), and MB of raw and pretreated *S. cerevisiae* increased with increasing solution pH value. At low pH values ($\text{pH} \leq 2$), protons occupy most of the binding sites of *S. cerevisiae* ($\text{H}^+ \gg \text{M}^{2+}$) and protons compete with cations. In contrast, as the pH value increases, the biosorbent surface takes more negative charges ($\text{M}^{2+} \gg \text{H}^+$), thus attracting greater cations. In addition, the ionizable side groups of ligands such as carboxyl, phosphate, imidazole, and amino groups are reacted with the positively charged ions [2,9,50–55].

Also, PZC points for raw and pretreated *S. cerevisiae* were found to be pH_{PZC} 5.07 and pH_{PZC} 7.50, respectively. At pH values below of isoelectric point of the biosorbent, the surface site of the *S. cerevisiae* is

positively charged and ion exchange mechanism plays an important role in the biosorption process. At pH values above of isoelectric point of the biosorbent, the surface site of the *S. cerevisiae* is negatively charged and physical mechanisms such as van der Waals forces attraction play an important role in the biosorption process. [34]. The PZC point for *S. cerevisiae* yeast in literature was found to be pH 4.50 [56].

However, the precipitated copper ions in hydroxide form ($\text{Cu}(\text{OH})^+$, $\text{Cu}(\text{OH})_2$, $\text{Cu}(\text{OH})_3^-$, $\text{Cu}_2(\text{OH})_2^{2+}$, and $\text{Cu}(\text{OH})_4^{2-}$) and the removal of Cu(II) ions from aqueous solution are contained both biosorption and precipitation mechanisms above pH 6.2 values [2,20]. In this study, it was also observed that precipitation was at above pH 6.0 for Cu(II) ions. According to Fig. 6, there is no significant difference in the biosorption capacities at pH 5 and above. Therefore, further experiments were conducted at pH 5 for Cu(II), Ni(II), and MB.

3.4. Effect of initial pollutant concentration on biosorption

The effect of different initial pollutant concentrations on the biosorption of Cu(II), Ni(II), and MB is given in Fig. 7(a) and (b). The biosorption capacities for Cu(II), Ni(II), and MB of raw and pretreated *S. cerevisiae* were found to be 0.99, 1.68, 2.38 and 2.18, 2.28, 2.37 mg/g at 25 mg/L initial pollutant concentration

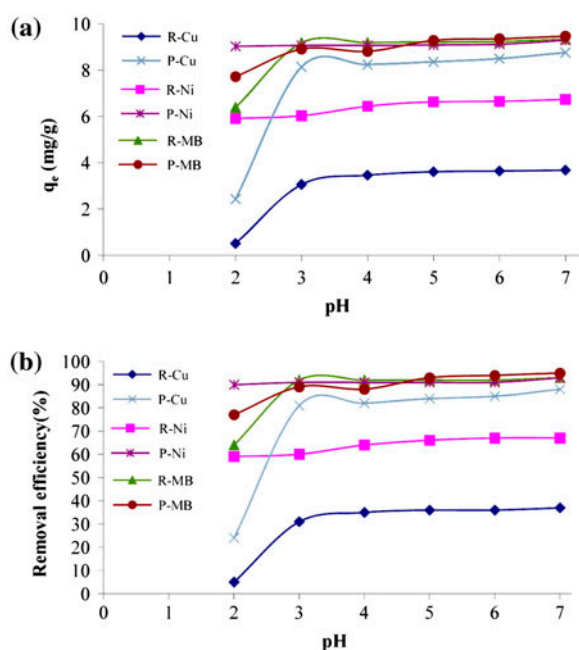


Fig. 6. Effect of pH (a) biosorption capacity, (b) removal efficiency (%).

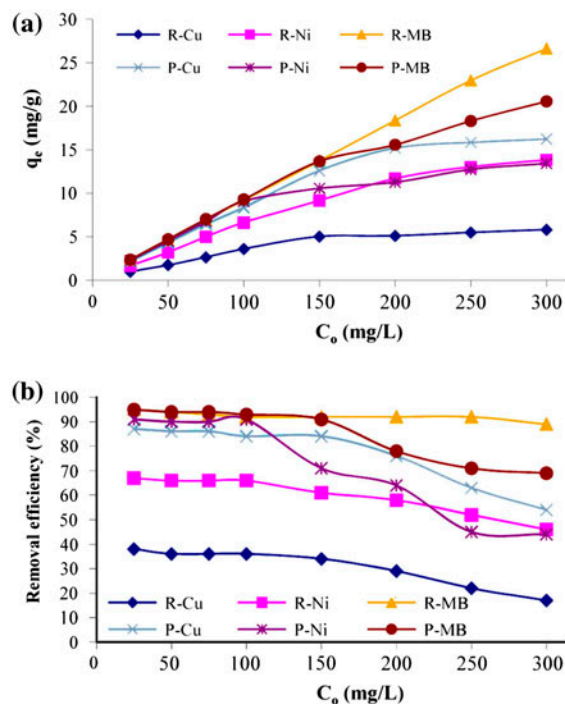


Fig. 7. Effect of initial pollutant concen. (a) biosorption capacity, (b) removal efficiency (%).

and as 5.82, 13.83, 26.62 and 16.22 13.42, 20.56 mg/g at 300 mg/L initial pollutant concentration, respectively. The biosorption capacity of raw and pretreated *S. cerevisiae* increased with increasing initial pollutant concentration and the removal efficiency slightly decreased at C_0 100 mg/L and above. This situation may be explained by saturation of the available binding sites on the *S. cerevisiae* [6,57,58].

Therefore, optimum initial pollutant concentrations for Cu(II), Ni(II), and MB were found to be 100, 100, 250 and 100, 100, 100 mg/L for raw and pretreated *S. cerevisiae*, respectively.

3.5. Effect of biosorbent dosage on biosorption

Batch experiments were carried out to optimize the biosorbent dosage for biosorption of the Cu(II), Ni(II), and MB and the results are given in Fig. 8 (a) and (b). As shown in Fig. 8(a) and (b), the removal efficiency and biosorbed pollutant amount (C_{bio}) increased with increasing biosorbent dosage as a result of the increase in the number of the active binding sites on the biosorbent. Several other investigators also reported the same trend of other biosorbent dosage effects on metal biosorption studies [9,59–61].

Therefore, the optimum dosage of raw and pretreated *S. cerevisiae* (X_0) for further experiments was selected as 10, 10, 10 and 7, 10, 10 g/L, respectively.

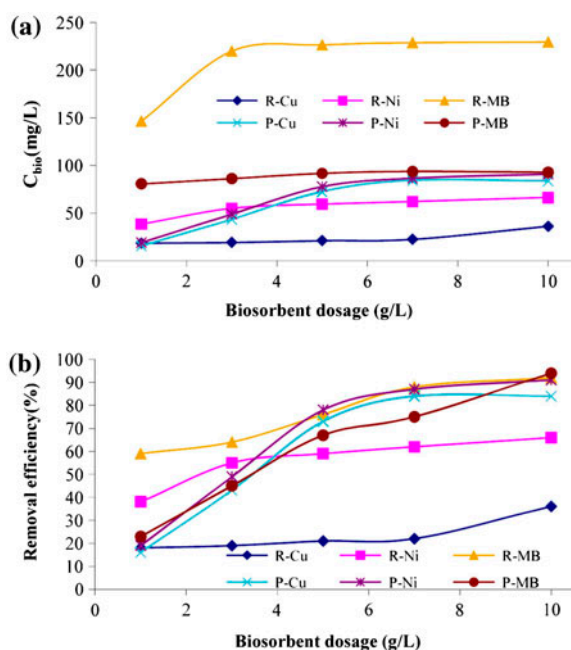


Fig. 8. Effect of biosorbent dosage (a) biosorbed pollutant amount, (b) removal efficiency (%).

3.6. Effect of contact time on biosorption and kinetic modeling

The effect of contact time on the biosorption of Cu(II), Ni(II), and MB onto raw and pretreated *S. cerevisiae* is given in Fig. 9(a) and (b). The biosorption capacity for Cu(II), Ni(II), and MB of raw *S. cerevisiae* increased substantially with increasing contact time up to 60, 60, and 90 min, respectively after which there was no significant change in biosorption.

50% of biosorption of Cu(II), Ni(II), and MB by pretreated *S. cerevisiae* was completed in 10, 60, and 5 min, respectively, and then it slowly reached equilibrium. Cu(II), Ni(II), and MB biosorption onto raw and pretreated *S. cerevisiae* occurred with sequential equilibrium steps. The very rapid surface sorption in the first stage and the slow intraparticle diffusion in the second stage occurred on the biosorption of Cu(II), Ni(II), and MB onto raw and pretreated *S. cerevisiae*. Van der Waals forces and ion exchange are effective in binding to *S. cerevisiae* surface of Cu(II), Ni(II), and MB (the first stage). Diffusion of Cu(II), Ni(II), and MB to the pores of the *S. cerevisiae* occurred in the second stage (intraparticle diffusion) [5,62].

Therefore, the optimum contact time was 1,440, 60, 90 and 1,440, 1,440, 1,440 min for Cu(II), Ni(II), and MB biosorption onto raw and pretreated *S. cerevisiae*, respectively.

The kinetic of Cu(II), Ni(II), and MB biosorption onto raw and pretreated *S. cerevisiae* was analyzed using the pseudo-first-order and pseudo-second-order kinetic models and intraparticle diffusion model. The

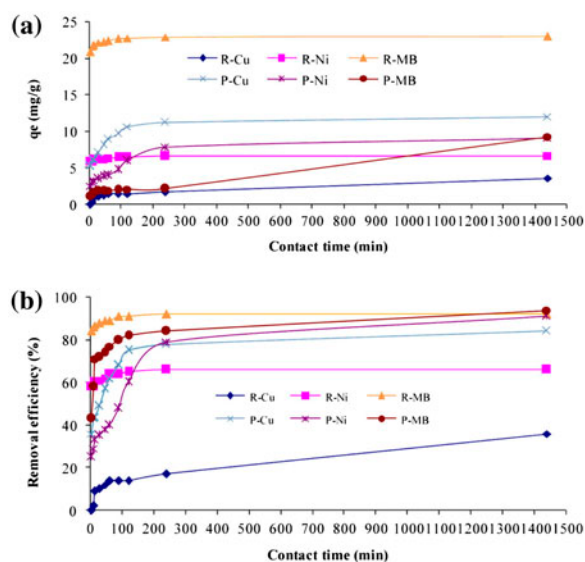


Fig. 9. Effect of contact time (a) biosorption capacity, (b) removal efficiency (%).

Table 4
Kinetic parameters for the biosorption of Cu(II), Ni(II), and MB onto raw and pretreated *S. cerevisiae*

	$q_{e,exp}$ (mg/g)	Pseudo-first-order kinetic model			Pseudo-second-order kinetic model				Intraparticle diffusion model		
		k_1	$q_{e,teo}$ (mg/g)	R^2	k_2	$q_{e,teo}$ (mg/g)	h (mg/g min)	R^2	k_d (mg/g min ^{0.5})	C	R^2
Raw <i>S. cerevisiae</i>											
Cu(II)	3.61	2.30×10^{-3}	2.93	0.609	1.82×10^{-3}	3.89	0.027	0.971	0.088	0.39	0.903
Ni(II)	6.64	0.018	0.95	0.968	0.068	6.65	3.007	1.000	0.021	6.03	0.544
MB	22.97	0.017	1.62	0.980	0.043	22.99	22.720	1.000	0.042	21.80	0.453
Pretreated <i>S. cerevisiae</i>											
Cu(II)	12.04	9.21×10^{-3}	6.09	0.931	4.65×10^{-3}	12.18	0.69	0.999	0.178	6.67	0.641
Ni(II)	9.09	7.14×10^{-3}	7.07	0.978	2.09×10^{-3}	9.39	0.18	0.997	0.191	2.80	0.820
MB	9.29	4.61×10^{-4}	7.71	0.478	3.61×10^{-4}	10.23	0.04	0.999	0.218	0.28	0.915

values of correlation coefficients (k_1, k_2, k_d), equilibrium biosorption capacities ($q_{e,teo}$), and initial sorption rate (h) in these models are given in Table 4. The correlation coefficients of the pseudo-second-order kinetic models were higher than the pseudo-first-order kinetic models and intraparticle diffusion models for Cu(II), Ni(II), and MB. In addition, calculated $q_{e,teo}$ values from pseudo-second-order kinetic models is very close to the experimental $q_{e,exp}$ values. These results suggest that the biosorption data are represented by pseudo-second-order kinetic model and the rate-controlling step of Cu(II), Ni(II), and MB biosorption onto raw and pretreated *S. cerevisiae* may be chemisorption process involving ion exchange or the complex formation between *S. cerevisiae* and Cu(II), Ni(II), and MB [23,63].

In addition, the intercept values (C) were greater than 0 in the present study. This showed that both intraparticle diffusion and boundary diffusion affected

the biosorption of Cu(II), Ni(II), and MB onto raw and pretreated *S. cerevisiae*.

3.7. Isotherm models

The experimental data fitted to Langmuir, Freundlich, and D–R isotherm models. The isotherm constants calculated from the Langmuir, Freundlich, and D–R isotherm models and the correlation coefficients are given in Table 5.

The correlation coefficients of Langmuir and Freundlich isotherms are quite high and experimental data of Cu(II) ions, Ni(II) ions, and MB are compatible with both Langmuir and Freundlich isotherms. Some researchers reported the experimental results obtained for single-metal biosorption onto *S. cerevisiae* yeast are generally compatible with both Langmuir and Freundlich models [9]. The applicability of both Langmuir

Table 5
Langmuir, Freundlich, and D–R isotherm model on biosorption of Cu(II), Ni(II), and MB onto raw and pretreated *S. cerevisiae*

	Langmuir				Freundlich			D–R				
	Q_{max} (mg/g)	b (L/mg)	R^2	R_L^*	k_F (L/g)	$1/n$	R^2	q_{D-R} (mol/g)	q_{D-R} (mg/g)	β (mol ² /J ²)	E (kJ/mol)	R^2
Raw <i>S. cerevisiae</i>												
Cu(II)	8.25	0.011	0.982	0.47	0.40	0.50	0.956	3.35×10^{-4}	21.27	6.64×10^{-9}	8.68	0.967
Ni(II)	21.39	0.013	0.995	0.43	0.84	0.57	0.977	7.87×10^{-4}	46.19	5.82×10^{-9}	9.27	0.975
MB	58.02	0.027	0.991	0.27	2.33	0.71	0.983	8.56×10^{-4}	320.06	4.87×10^{-9}	10.13	0.976
Pretreated <i>S. cerevisiae</i>												
Cu(II)	19.45	0.053	0.984	0.16	2.99	0.37	0.929	8.14×10^{-4}	51.88	4.63×10^{-9}	10.40	0.964
Ni(II)	13.26	0.134	0.971	0.07	3.72	0.26	0.934	4.68×10^{-4}	27.43	3.23×10^{-9}	12.45	0.974
MB	21.02	0.117	0.988	0.08	4.22	0.35	0.969	1.44×10^{-4}	53.84	2.51×10^{-9}	14.12	0.966

* R_L value calculated in 100 mg/L initial pollutant concentrations is given.

and Freundlich isotherms on the biosorption of Cu(II), Ni(II), and MB onto raw and pretreated *S. cerevisiae* shows that biosorption occurs under monolayer and heterogeneous surfaces [64]. The maximum biosorption capacities of the raw and pretreated *S. cerevisiae* for the removal of Cu(II), Ni(II), and MB have been compared with those of other biosorbents reported in literature and the values of maximum biosorption capacities (Q_{\max}) have been presented in Table 6. The values are based on the maximum biosorption capacity obtained from Langmuir isotherm.

The calculated R_L values range between 0 and 1, indicating that the biosorption of Cu(II), Ni(II), and MB onto raw and pretreated *S. cerevisiae* is favorable. The $1/n$ heterogeneity factor was found to be between 0 and 1, suggesting relatively strong biosorption of Cu(II), Ni(II), and MB onto the surface raw and pretreated *S. cerevisiae*.

The mean free energy (E ; kJ/mol) values calculated from the D–R isotherm model were also determined between 8 and 16 kJ/mol. It explains that the biosorption is mainly a chemical process through ion exchange.

3.8. Evaluation of thermodynamic parameters

The values of ΔG , ΔH , and ΔS obtained from this plot are given in Table 7. The negative values of ΔG

and ΔH indicate that the biosorption processes are feasible, spontaneous, and exothermic in nature (Table 7). The biosorption capacity of raw and pretreated *S. cerevisiae* decreased with increasing temperature. The reason for this may be due to the damage of some active binding sites on the *S. cerevisiae* [9,51]. The positive value of ΔS also shows the increase in randomness at the solid/liquid interface during the biosorption.

3.9. Desorption studies

Desorption is very much necessary when the preparation and generation of biosorbent is costly. A successful desorption process depends on the mechanism of biosorption, the type of biosorbent, and the proper selection of desorbents. The selected desorbents for desorption process must be non-damaging to the biosorbent, less costly, eco-friendly, and efficient [75].

In the present investigation, two different desorbent solutions (laundry detergent and 0.1M HCl, which does not cause the precipitation with any metal) were used for desorption of Cu(II) and Ni(II) metal ions from the raw and pretreated *S. cerevisiae*. 0.1M HCl and 0.1M NaOH desorbent solutions were also investigated for desorption of MB dye from the raw and pretreated *S. cerevisiae* yeast. Desorption ratio was given as [2,76]:

Table 6
The maximum biosorption capacities of various biosorbents

Biosorbent	Metal/dye	Q_{\max} (mg/g)	References
Raw <i>S. cerevisiae</i>	Cu(II)	8.25	In this study
Pretreated <i>S. cerevisiae</i>	Cu(II)	19.45	In this study
<i>S. cerevisiae</i>	Cu(II)	10.27	[2]
Caustic- <i>S. cerevisiae</i>	Cu(II)	27.32	[2]
<i>S. cerevisiae</i>	Cu(II)	2.59	[65]
Immobilize <i>Arthrobacter</i> sp.	Cu(II)	32.60	[66]
<i>Sargassum</i>	Cu(II)	38	[67]
Raw <i>S. cerevisiae</i>	Ni(II)	21.39	In this study
Pretreated <i>S. cerevisiae</i>	Ni(II)	13.26	In this study
<i>S. cerevisiae</i>	Ni(II)	9.01	[68]
<i>S. cerevisiae</i>	Ni(II)	46.30	[51]
<i>Yarrowia lipolytica</i>	Ni(II)	138.88	[69]
<i>Yarrowia lipolytica</i>	Ni(II)	112.35	[69]
Cone biomass of <i>T. orientalis</i>	Ni(II)	12.42	[70]
Raw <i>S. cerevisiae</i>	Methylene Blue	58.02	In this study
Pretreated <i>S. cerevisiae</i>	Methylene Blue	21.02	In this study
<i>Rhizopus arrhizus</i>	Methylene Blue	370.30	[71]
<i>A. fumigates</i>	Methylene Blue	125	[72]
<i>A. niger</i>	Methylene Blue	18.54	[73]
<i>A. wentii</i>	Methylene Blue	3.30	[74]

Table 7

Thermodynamic parameters in the biosorption of Cu(II), Ni(II), and MB onto raw and pretreated *S. cerevisiae*

	ΔH (kJ/mol)	ΔS (kJ/molK)	ΔG^* (kJ/mol)	R^2
Raw <i>S. cerevisiae</i>				
Cu(II)	-37.90	-0.09	-11.53	0.914
Ni(II)	-28.70	-0.06	-11.20	0.841
MB	-23.10	-0.02	-17.24	0.789
Pretreated <i>S. cerevisiae</i>				
Cu(II)	-16.10	-0.001	-16.39	0.605
Ni(II)	-0.80	0.05	-15.45	0.011
MB	-5.46	0.04	-17.18	0.940

* ΔG value calculated in 293 K temperature is given.

$$\text{The desorption ratio} = \frac{\text{amount of pollutant desorbed}}{\text{amount of pollutant biosorbed}} \times 100 \quad (16)$$

The percentage of Cu(II), Ni(II), and MB released after desorption treatment is given in Fig. 10.

HCl is an effective desorbent for recovery of MB and Cu(II). The desorption process of HCl is based on the ion exchange between HCl protons and cations in binding sites of *S. cerevisiae*. Laundry detergent is a good desorbent in the recovery of Cu(II) ions. This condition may be explained on the basis of ion exchange between the Cu(II) ions and the sodium in the laundry detergent.

3.10. Effect of ionic strength (IS) on biosorption

The biosorption capacity was strongly affected by the concentrations and structural characteristics of the electrolyte ionic species added to the dye solution [77]. The effect of ionic strength on Cu(II), Ni(II), and MB biosorption was studied by changing IS from 0.01 to 1.00 M NaCl at determined optimum conditions in the present study for each metal and dye. The effect of inorganic salt (NaCl) on removal efficiency of Cu(II), Ni(II), and MB from aqueous solution is presented in Table 8.

The biosorption of Cu(II) on raw and pretreated *S. cerevisiae* decreased with increasing NaCl concentration. This condition can be explained as the result of an electrostatic competition of Na^+ ions with Cu(II) metal ions at the binding sites of biosorbent. In contrast, the presence of NaCl in aqueous solution increased the biosorption of Ni(II) and MB. The salt causes an increase in the degree of dissociation of the molecules by facilitating the protonation. This

situation has been effective on the biosorption of Ni(II) and MB [77–79].

3.11. Biosorption selectivity of biosorbent

In general, the presence of competing ions in aqueous solution causes a decrease of biosorption efficiency. The degree of this decrease depends on the quantity of the functional groups on biosorbent, the species and concentration of ions, ionic charge, and semi-diameter of ions [2]. The biosorption selectivity of raw and pretreated *S. cerevisiae* was investigated under the following conditions: C_0 100 mg/L, pH 5.0, contact time: 1,440 min, and X_0 : 10 g/L. The relative biosorption of Cu(II), Ni(II), and MB onto raw and pretreated *S. cerevisiae* in binary solution were calculated from [80]:

$$A_r = \frac{[q_t]_B}{[q_t]_S} \quad (17)$$

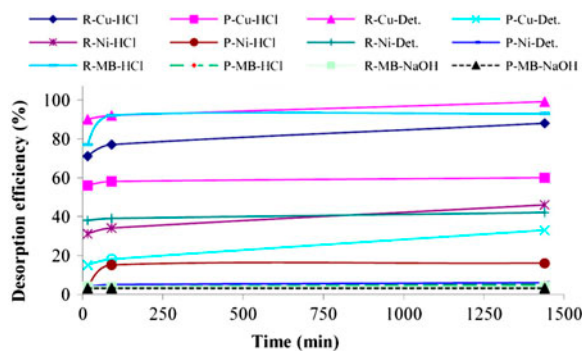


Fig. 10. The desorption efficiency with different desorbents for Cu(II), Ni(II), and MB.

Table 8
Ionic strength effect on Cu(II), Ni(II), and MB biosorption and Cu(II), Ni(II), and MB selectivity of *S. cerevisiae*

Effect of IS NaCl concentration (mol/L)	Removal efficiency (%)					
	Raw <i>S. cerevisiae</i>			Pretreated <i>S. cerevisiae</i>		
	Cu(II)	Ni(II)	MB	Cu(II)	Ni(II)	MB
0	36	64	91	84	91	94
0.01	24	88	42	78	90	38
0.05	10	88	45	56	89	42
0.10	7	80	49	31	82	51
0.50	0	72	96	11	78	93
1.00	0	69	97	2	76	97

Cu(II), Ni(II), and MB selectivity of <i>S. cerevisiae</i> Biosorbent	Mono component study			Multi component study		
	Cu(II)	Ni(II)	MB	Cu(II)	Ni(II)	MB
	Raw <i>S. cerevisiae</i>	36	66	92	21	41
Pretreated <i>S. cerevisiae</i>	84	91	94	58	64	85

	Relative biosorption (A_r)		
	Cu(II)	Ni(II)	MB
	Raw <i>S. cerevisiae</i>	0.58	0.62
Pretreated <i>S. cerevisiae</i>	0.69	0.70	0.92

	Biosorption selectivity (S)		
	$S = \frac{A_{rMB}}{A_{rCu}}$	$S = \frac{A_{rMB}}{A_{rNi}}$	$S = \frac{A_{rNi}}{A_{rCu}}$
	Raw <i>S. cerevisiae</i>	1.41	1.32
Pretreated <i>S. cerevisiae</i>	1.33	1.32	1.01

where $[q_t]_B$ and $[q_t]_S$ are the biosorption capacities in binary solution and single solution at time t , respectively. Also, biosorption selectively in the binary solution is defined in [80]:

$$S = \frac{(A_r)_1}{(A_r)_2} \quad (18)$$

The removal efficiencies (%), relative biosorption (A_r), and biosorption selectivity of Cu(II), Ni(II), and MB from multi component aqueous system are given in Table 8.

According to Table 8, the affinity of raw and pretreated *S. cerevisiae* is determined as MB > Ni(II) > Cu(II). The relative biosorption values of Cu(II) and Ni(II) at the equilibrium are very close. Under the same conditions, the removal efficiencies in single component system of Cu(II), Ni(II), and MB by raw and pretreated *S. cerevisiae* were found as 36, 66, 92 and 84, 91, 94%, respectively. This situation can be explained that

competition of Cu(II), Ni(II) ions, and MB dye for the limited binding sites on biosorbent.

3.12. Effect of binary component on biosorption

The equilibrium isotherms, kinetics, and thermodynamic parameters were determined for the mono component systems to predict the nature of biosorption of Cu(II), Ni(II), and MB onto raw and pretreated *S. cerevisiae*. However, the real wastewaters contains more metal compounds and dye complexes[81]. Nowadays, only limited information is available on the competition of biosorption, including *S. cerevisiae* [9]. Therefore, to simulate the real wastewater conditions, the binary component biosorption of the Cu(II)–Ni(II), Ni(II)–MB, and Cu(II)–MB were studied.

Generally, in binary component biosorption studies, there are three possible types of behaviors such as synergism, antagonism, and non-interaction. In this study, the binary biosorption onto raw and pretreated

S. cerevisiae exhibited antagonistic biosorption for each pollutant. The biosorption capacities of raw and pretreated *S. cerevisiae* for dominant pollutant decreased with increasing the competing pollutant concentration. The most logical reason for the antagonistic action could be explained as the competition between like-charged species for binding sites of the *S. cerevisiae* cells [82,83]. The multi component isotherm using only the parameters of mono component isotherm may not definitely describe the antagonistic interactions biosorption behavior of pollutant mixtures. For that reason, modified isotherms related to the individual isotherm parameters and the correction factors may give accuracy predication [15,80]. The modified Langmuir and extended Freundlich isotherm models for binary component systems are given by the following equations, respectively [15,80]:

$$q_{ei} = \frac{Q_i^0 b_i \frac{C_{ei}}{\eta_{li}}}{1 + \sum_{j=1}^N b_j \frac{C_{ej}}{\eta_{lj}}} \quad (19)$$

$$q_{e1} = \frac{k_{F1}(C_{e1})^{(\eta_{11}+x_1)}}{(C_{e1})^{x_1} + y_1(C_{e2})^{z_1}} \quad (20)$$

$$q_{e2} = \frac{k_{F2}(C_{e2})^{(\eta_{21}+x_2)}}{(C_{e2})^{x_2} + y_2(C_{e1})^{z_2}} \quad (21)$$

α and β values are the Langmuir isotherm constants of the primary component for binary component systems. x , y , and z values are the Freundlich and Langmuir isotherm constants of the primary component for binary component systems. An interaction term, α , is a characteristic of each species and depends on the concentrations of the other components. The α value greater than 1 indicates that the modified Langmuir isotherm models related to the individual isotherm parameter could be used to predict the binary component biosorption [15,80]. The parameters of binary component biosorption isotherms are given in Table 9.

Table 9
Isotherm models for binary component biosorption of Cu(II), Ni(II), and MB

Biosorbent	Isotherm	Parameters	Binary component studies	
Raw <i>S. cerevisiae</i>			Cu(II)–Ni(II) studies	
			Cu(II)	Ni(II)
	Langmuir isotherm	α	1.57	1.81
		β	1.86	2.41
	Freundlich isotherm	x	–0.07	0.30
		y	0.02	0.28
		z	0.78	0.69
			Ni(II)–MB studies	
			Ni(II)	MB
	Langmuir isotherm	α	1.28	1.23
β		1.32	1.95	
Freundlich isotherm	x	1.07	0.62	
	y	5.62	0.73	
	z	0.69	0.58	
Pretreated <i>S. cerevisiae</i>			Cu(II)–Ni(II) studies	
	Langmuir isotherm	α	1.64	0.32
		β	2.50	0.20
	Freundlich isotherm	x	0.96	0.99
		y	3.93	0.75
		z	0.59	1.05
			Cu(II)–MB studies	
	Langmuir isotherm	α	1.16	1.28
		β	1.90	1.34
	Freundlich isotherm	x	1.36	0.79
y		0.68	0.98	
z		0.43	0.75	

The biosorption isotherms for binary biosorption of Cu(II)–Ni(II), Ni(II)–MB, and Cu(II)–MB onto raw and pretreated *S. cerevisiae* are given in Figs. 11–14. As shown in Figs. 11–14, the biosorption capacities of each metal or dye in binary component biosorption were lower than those in single component biosorption.

In binary component biosorption process, the two pollutants competed for the biosorption sites. These results are compatible with results obtained from ionic selectivity of raw and pretreated *S. cerevisiae* biosorbents.

3.13. Biosorption mechanism

The biosorption process includes different mechanisms[80]. The pH is effective in the surface charge of the biosorbent and the dissociation of functional groups on the active sites of the biosorbent[80,84]. Also, PZC point is an effective factor in the determination of surface charge of the biosorbent. FT-IR analysis showed that the fundamental organic functional groups, such as carboxyl, amino/hydroxyl, and phosphoryl, are located on the cell wall of *S. cerevisiae* [40]. Therefore, the negative sites of *S. cerevisiae*, such as

carboxyl and phosphoryl groups, played a role in Cu (II), Ni(II), and MB biosorption. A high biosorption capacity was observed for MB than Cu(II) and Ni(II) in single and binary solutions. The chemical structures, the number and position of the functional groups, dimensions of the organic chains, and the molecular size of Cu(II), Ni(II), and MB may have caused the difference in biosorption capacity and antagonistic interactions between the Cu(II), Ni(II), and MB [15].

4. Conclusions

The results of the present study indicate that the raw and detergent-pretreated *S. cerevisiae* have a significant potential for the removal of Cu(II) and Ni(II) metal ions and MB dye from the aqueous solutions. The structure of raw and pretreated *S. cerevisiae* were characterized by FT-IR, XRD, and SEM analyses. Pretreatment of the *S.cerevisiae* with detergent increased the biosorption capacity of *S. cerevisiae* when compared with the raw *S. cerevisiae*. The highest removal efficiencies obtained for Cu(II), Ni(II), and MB biosorption onto detergent-pretreated *S. cerevisia* were 84,

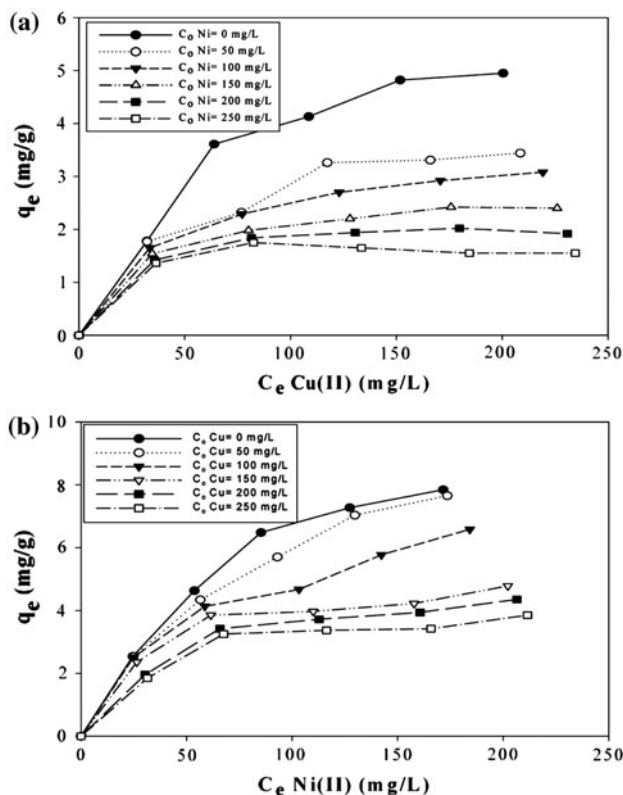


Fig. 11. Biosorption isotherms of Cu(II)–Ni(II) binary biosorption onto raw *S. cerevisiae* (t : 20°C, X_0 : 10 g/L, pH 5.0).

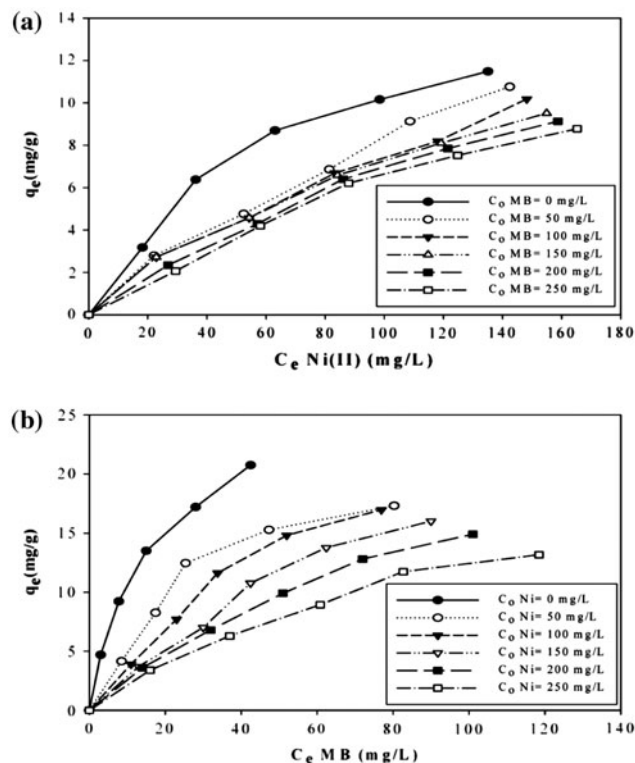


Fig. 12. Biosorption isotherms of Ni(II)–MB binary biosorption onto raw *S. cerevisiae* (t : 20°C, X_0 : 10 g/L, pH 5.0).

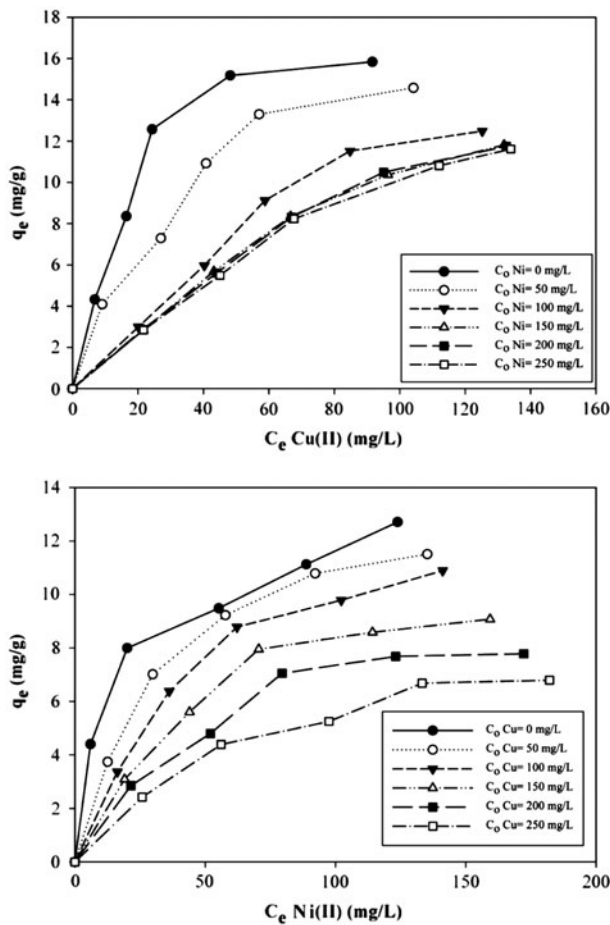


Fig. 13. Biosorption isotherms of Cu(II)–Ni(II) binary biosorption onto pretreated *S. cerevisiae* (t : 20°C, X_0 : 10 g/L, pH 5.0).

91, and 94%, respectively, whereas the highest removal efficiency achieved using raw *S. cerevisiae* was found to be 36, 66, and 92%. The experimental data were analyzed using Langmuir, Freundlich, and D–R isotherm models. The equilibrium data for Cu(II), Ni(II), and MB are compatible with both the Langmuir and Freundlich isotherm models.

The pseudo-second-order kinetic model is the best kinetic model for biosorption of Cu(II), Ni(II), and MB onto raw and pretreated *S. cerevisiae*. Kinetic data were also analyzed through the intraparticle diffusion model. According to results obtained for this model, the biosorption process was realized by a combination of intraparticle diffusion model and boundary layer diffusion model. Thermodynamic parameters show that the biosorption of Cu(II), Ni(II), and MB is exothermic and spontaneous in nature. Binary component biosorption studies showed that removal efficiency of the dominant pollutant from the aqueous

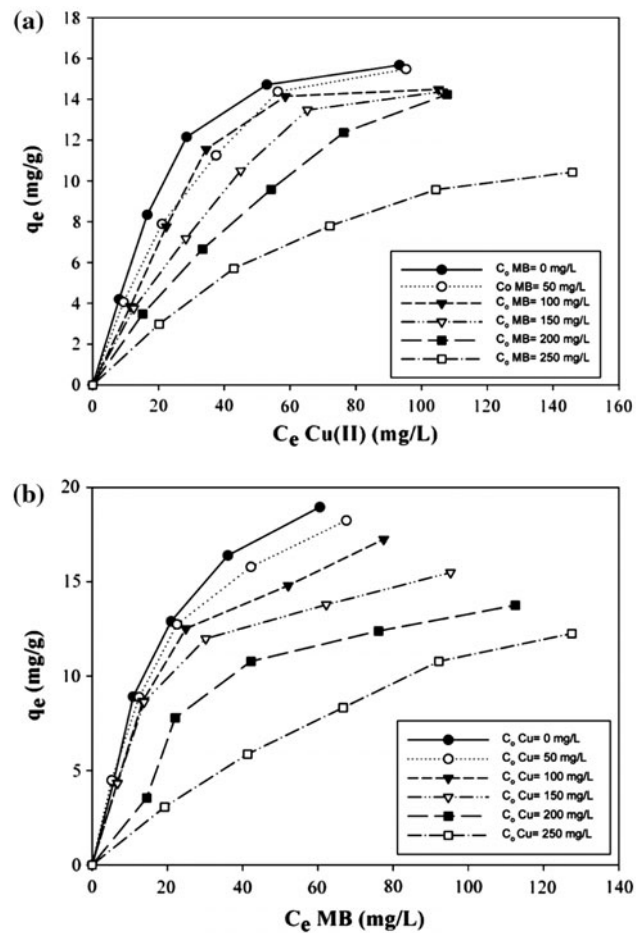


Fig. 14. Biosorption isotherms of Cu(II)–MB binary biosorption onto pretreated *S. cerevisiae* (t : 20°C, X_0 : 10 g/L, pH 5.0).

solutions decreased by the presence of the competing pollutant.

Based on all these results, the raw and detergent-pretreated *S. cerevisiae* can be preferred as alternative biosorbents in large-scale plants for single and simultaneous removal of Cu(II), Ni(II), and MB from contaminated aqueous ecosystems as they can be easily obtained and are inexpensive, sustainable, efficient, and non-pathogenic.

Acknowledgment

This work is supported by the Scientific Research Project Fund of Cumhuriyet University under the project number M-326.

References

- [1] M. Sarioglu, U.A. Atay, Removal of Methylene Blue by using biosolid, *Global Nest J.* 8 (2006) 113–120.

- [2] Y. Zhang, W. Liu, M. Xu, F. Zheng, M. Zhao, Study of mechanisms of Cu(II) biosorption by ethanol/caustic-pretreated baker's yeast biomass, *J. Hazard. Mater.* 178 (2010) 1085–1093.
- [3] M.M. Montazer-Rahmati, P. Rabbani, A. Abdolali, A.R. Keshtkar, Kinetics and equilibrium studies on biosorption of cadmium, lead, and nickel ions from aqueous solutions by intact and chemically modified brown algae, *J. Hazard. Mater.* 185 (2011) 401–407.
- [4] A. Lyer, K. Mody, B.K. Jha, Biosorption of heavy metals by a marine bacterium, *Marine Pollut.* 50 (2005) 175–179.
- [5] H. Pahlavanzadeh, A.R. Keshtkar, J. Safdari, Z. Abadi, Biosorption of nickel(II) from aqueous solution by brown algae: Equilibrium, dynamic and thermodynamic studies, *J. Hazard. Mater.* 175 (2010) 304–310.
- [6] Z. Aksu, G.A. Donmez, A comparative study on the biosorption characteristics of some yeasts for Remazol Blue reactive dye, *Chemosphere* 50 (2003) 1075–1083.
- [7] O.S. Lawal, A.R. Sanni, I.A. Ajayi, O.O. Rabiou, Equilibrium, thermodynamic and kinetic studies for the biosorption of aqueous lead(II) ions onto the seed husk of *Calophyllum inophyllum*, *J. Hazard. Mater.* 177 (2010) 829–835.
- [8] Z. Aksu, Application of biosorption for the removal of organic pollutants: A review, *Process Biochem.* 40 (2005) 997–1026.
- [9] J. Wang, J.C. Chen, Biosorption of heavy metals by *Saccharomyces cerevisiae*: A review, *Biotech. Adv.* 24 (2006) 427–451.
- [10] J. Wang, J.C. Chen, Biosorbents for heavy metals removal and their future, *Biotech. Adv.* 27 (2009) 195–226.
- [11] A. Tassist, H. Lounici, N. Abdi, N. Mameri, Equilibrium, kinetic and thermodynamic studies on aluminum biosorption by a mycelial biomass (*Streptomyces rimosus*), *J. Hazard. Mater.* 183 (2010) 35–43.
- [12] A. Malik, Metal bioremediation through growing cells, *Environ. Int.* 30 (2004) 267–278.
- [13] A. Kapoor, T. Viraraghavan, Fungi biosorption—An alternative treatment option for heavy metal bearing wastewaters: A review, *Bioresour. Technol.* 53 (1995) 195–206.
- [14] Y. Cao, Z. Liu, G. Cheng, X. Jing, H. Xu, Exploring single and multi-metal biosorption by immobilized spent *Tricholoma lobayense* using multi-step response surface methodology, *Chem. Eng. J.* 164 (2010) 183–195.
- [15] J.F. Gao, J.H. Wang, C. Yang, S.Y. Wang, Y.Z. Peng, Binary biosorption of acid red 14 and reactive red 15 onto acid treated Okara: Simultaneous spectrophotometric determination of two dyes using partial least squares regression, *Chem. Eng. J.* 171 (2011) 967–975.
- [16] A. Kapoor, T. Viraraghavan, Biosorption of heavy metals on *Aspergillus niger*: Effect of pretreated, *Bioresour. Technol.* 63 (1998) 109–113.
- [17] H. Yazici, M. Kilic, M. Solak, Biosorption of copper(II) by *Marrubium globosum* subsp. *Globosum* leaves powder: Effect of chemical pretreated, *J. Hazard. Mater.* 151 (2008) 669–675.
- [18] H. Ucu, Y.K. Bayhan, Y. Kaya, Kinetic and thermodynamic studies of the biosorption of Cr(VI) by *Pinus sylvestris* Linn, *J. Hazard. Mater.* 153 (2008) 52–59.
- [19] K.R. Hall, L.C. Eagleton, A. Acrivos, T. Vermeulen, Pore and solid diffusion kinetics in fixed-bed adsorption under constant pattern conditions, *Ind. Eng. Chem. Fundam.* 5 (1966) 212–223.
- [20] C.H. Wu, Studies of equilibrium and thermodynamics of the adsorption Cu(II) onto as-produced and modified carbon nanotubes, *J. Colloid Interface Sci.* 311 (2007) 338–346.
- [21] A. Sari, D. Mendil, M. Tuzen, M. Soylak, Biosorption of Cd(II) and Cr(III) from aqueous solution by moss (*Hylocomium splendens*) biomass: equilibrium, kinetic and thermodynamic Studies, *Chem. Eng. J.* 144 (2008) 1–9.
- [22] M.M. Dubinin, E.D. Zaverina, L.V. Radushkevich, Sorption and structure of active carbons, I. adsorption of organic vapors, *Zh. Fiz. Khim.* 21 (1947) 1351–1362.
- [23] P. Lodeiro, J.L. Barriada, R. Herrero, M.E. Sastre de Vicente, The marine macroalga *Cystoseira baccata* as biosorbent for cadmium(II) and lead(II) removal: Kinetic and equilibrium studies, *Environ. Pollut.* 142 (2006) 264–273.
- [24] A. Sari, M. Tuzen, Biosorption of Pb(II) and Cd(II) from aqueous solution using green alga (*Ulva lactuca*) biomass, *J. Hazard. Mater.* 152 (2008) 302–308.
- [25] Y.S. Ho, G. McKay, Pseudo-second order model for sorption processes, *Process Biochem.* 34 (1999) 451–465.
- [26] A. Murugesan, L. Ravikumar, V. SathyaSelvaBala, P. SenthilKumar, T. Vidhyadevi, S. Dinesh, S. Kirupha, S.S. Kalainani, S. Krithiga, S. Sivanesan, Removal of Pb(II), Cu(II) and Cd(II) ions from aqueous solution using polyazomethineamides: Equilibrium and kinetic approach, *Desalination* 271 (2011) 199–208.
- [27] A. Sari, M. Tuzen, M. Soylak, Adsorption of Pb(II) and Cr(III) from aqueous solution on Celtek clay, *J. Hazard. Mater. B* 144 (2007) 41–46.
- [28] A. Sari, M. Tuzen, Equilibrium, thermodynamic and kinetic studies on aluminum biosorption from aqueous solution by brown algae (*Padina pavonica*) biomass, *J. Hazard. Mater.* 171 (2009) 973–979.
- [29] H. Nolle, M. Roels, Y. Lutgen, P. Ash, P. Van Der Meeren, W. Verstraete, Removal of PCBs from wastewater using fly ash, *Chemosphere* 53 (2003) 655–665.
- [30] N. Chubar, J.R. Carvalho, M.J.N. Correia, Heavy metals biosorption on cork biomass: Effect of the pre-treatment, *Colloids Surf. A* 238 (2004) 51–58.
- [31] T. Akar, S. Tunali, Biosorption characteristics of *Aspergillus flavus* biomass for removal of Pb(II) and Cu(II) ions from an aqueous solution, *Bioresour. Technol.* 97(15) (2006) 1780–1787.
- [32] C.L. Brierley, Bioremediation of metal-contaminated surface and groundwater, *Geomicrobiol. J.* 8 (1990) 201–223.
- [33] J.P. Chen, L. Yang, Chemical modification of *Sargassum* sp. for prevention of organic leaching and enhancement of uptake during metal biosorption, *Ind. Eng. Chem. Res.* 44(26) (2005) 9931–9942.
- [34] I. Kiran, T. Akar, S. Tunali, Biosorption of Pb(II) and Cu(II) from aqueous solutions by pretreated biomass of *Neurospora crassa*, *Process Biochem.* 40 (2005) 3550–3558.
- [35] Z. Al-Qodah, Biosorption of heavy metal ions from an aqueous solution by activated sludge, *Desalination* 196 (2006) 164–176.
- [36] G. Yan, T. Viraraghavan, Effect of pretreated on the bioadsorption of heavy metals on *Mucor rouxii*, *Water SA.* 26 (2000) 119–123.
- [37] P. Sar, S.K. Kazy, R.K. Asthana, D. Singh, Metal adsorption and desorption by iyophilized *Pseudomonas aeruginosa*, *Int. Biodegrad. Biodegrad.* 44 (1999) 101–110.
- [38] M. Bansal, U. Garg, D. Singh, V.K. Garg, Removal of Cr(VI) from aqueous solutions using pre-consumer processing agricultural waste: A case study of rice husk, *J. Hazard. Mater.* 162 (2009) 312–320.
- [39] M. Fereidouni, A. Daneshi, H. Younesi, Biosorption equilibria of binary Cd(II) and Ni(II) systems onto *Saccharomyces cerevisiae* and *Ralstonia eutropha* cells: Application of response surface methodology, *J. Hazard. Mater.* 168 (2009) 1437–1448.
- [40] J.X. Yu, M. Tong, X.M. Sun, B.H. Li, Enhanced and selective adsorption of Pb(II) and Cu(II) by EDTA-modified biomass of baker's yeasts, *Bioresour. Technol.* 99 (2009) 2588–2593.
- [41] A. Selatnia, A. Boukazoula, N. Kechid, M.Z. Bakhti, A. Chergui, Biosorption of Fe(III) from aqueous solution by a bacterial dead *Streptomyces rimosus* biomass, *Process Biochem.* 39 (2004) 1643–1651.
- [42] R. Nadeem, T.M. Ansari, A.M. Khalid, Fourier transform infrared spectroscopic characterization and optimization of Pb(II) biosorption by fish (*Labeo rohita*) scales, *J. Hazard. Mater.* 156 (2008) 64–73.
- [43] Z. Aksu, Y. Sağ, T. Kutsal, The biosorption of copper(II) by *Chlorella vulgaris* and *Zoogloea ramigera*, *Environ. Technol.* 13 (1992) 579–586.

- [44] Y. Zhang, C. Fan, Q. Meng, Z. Diao, L. Dong, X. Peng, S. Ma, Q. Zhou, Biosorption of Pb(II) by *Saccharomyces cerevisiae* in static and dynamic adsorption tests, *Bull. Environ. Contam. Toxicol.* 83 (2009) 708–712.
- [45] D. Shu-juan, W. De-zhou, Z. Dong-qin, J. Chun-yun, W. Yu-juan, L. Wen-gang, Removing cadmium from electroplating wastewater by waste *Saccharomyces cerevisiae*, *Trans. Nonferrous Met. Soc. China* 18 (2008) 1008–1013.
- [46] Y. Göksungur, S. Üren, U. Güvenc, Biosorption of copper ions by caustic treated waste baker's yeast biomass, *Turk. J. Biol.* 27 (2003) 23–29.
- [47] P.A. Marques, H.M. Pinheiro, J.A. Teixeira, M.F. Rosa, Removal efficiency of Cu(II), Cd(II), Pb(II) by waste brewery biomass: pH and cation association effects, *Desalination* 124 (1999) 137–144.
- [48] C.P. Huang, C.P. Huang, A.L. Morehart, The removal of Cu (II) from dilute aqueous solutions by *Saccharomyces cerevisiae*, *Water Res.* 24 (1999) 433–439.
- [49] A. Esposito, F. Pagnanelli, F. Veglio, pH-related equilibria models for biosorption in single metal systems, *Chem. Eng. Sci.* 57 (2002) 307–313.
- [50] S. Schiewer, B. Volesky, Modelling of proton-metal ion exchange in biosorption, *Environ. Sci. Technol.* 29 (1995) 3049–3058.
- [51] A. Özer, D. Özer, Comparative study of the biosorption of Pb(II), Ni(II) and Cr(VI) ions onto *S. cerevisiae*: Determination of biosorption heats, *J. Hazard. Mater. B* 100 (2003) 219–229.
- [52] M. Mapolelo, N. Torto, Trace enrichment of metal ions in aquatic environments by *Saccharomyces cerevisiae*, *Talanta* 64 (2004) 39–47.
- [53] L.N.L. Vianna, M.C. Andrade, J.R. Nicoli, Screening of waste biomass from *Saccharomyces cerevisiae*, *Aspergillus oryzae* and *Bacillus lentus* fermentations for removal of Cu, Zn and Cd by biosorption, *World J. Microbiol. Biotechnol.* 16 (2000) 437–440.
- [54] N.S. Maurya, N.S.A.K. Mittal, P. Cornel, E. Rother, Biosorption of dyes using dead macro fungi: Effect of dye structure, ionic strength and pH, *Bioresour. Technol.* 97 (2006) 512–521.
- [55] P. Kaushik, A. Malik, Fungal dye decolourization: Recent advances and future potential, *Environ. Int.* 35 (2009) 127–141.
- [56] Y. Tian, C. Ji, M. Zhao, M. Xu, Y. Zhang, R. Wang, Preparation and characterization of baker's yeast modified by nano-Fe₃O₄: Application of biosorption of methyl violet in aqueous solution, *Chem. Eng. J.* 165 (2010) 474–481.
- [57] Y.S. Ho, G. McKay, The kinetics of sorption of divalent metals onto Sphagnum moss Peat, *Water Res.* 34 (2000) 735–742.
- [58] K. Kumari, T.E. Abraham, Biosorption of anionic textile dyes by nonviable biomass of fungi and yeast, *Bioresour. Technol.* 98 (2007) 1704–1710.
- [59] P. Vasudevan, V. Padmavathy, S.C. Dhingra, Biosorption of monovalent and divalent ions on baker's yeast, *Bioresour. Technol.* 82 (2002) 285–289.
- [60] P. Vasudevan, V. Padmavathy, S.C. Dhingra, Kinetics of biosorption of cadmium on baker's yeast, *Bioresour. Technol.* 89 (2003) 281–287.
- [61] A. Çabuk, T. Akar, S. Tunalı, S. Gedikli, Biosorption of Pb (II) by industrial strain of *Saccharomyces cerevisiae* immobilized on the biomatrix of cone biomass of *Pinus nigra*: Equilibrium and mechanism analysis, *Chem. Eng. J.* 131 (2007) 293–300.
- [62] M. Bustard, G. McMullan, A.P. McHale, Biosorption of textile dyes by biomass derived from *Kluyveromyces marxianus* IMB3, *Bioprocess Eng.* 19 (1998) 427–430.
- [63] I. Smiciklas, S. Dimovic, I. Plecas, M. Mitric, Removal of Co (II) from aqueous by hydroxyapatite, *Water Res.* 40 (2006) 2267–2274.
- [64] Z. Aksu, Biosorption of reactive dyes by dried activated sludge: Equilibrium and kinetic modelling, *Biochem. Eng. J.* 7 (2001) 79–84.
- [65] C. Corneliu, D. Mariana, Biosorption of copper(II) ions from aqua solutions using dried yeast biomass, *Colloids Surf. A* 335 (2009) 181–188.
- [66] S.H. Hasan, P. Srivastava, Batch and continuous biosorption of Cu²⁺ by immobilized biomass of *Arthrobacter sp.*, *J. Environ. Manage.* 90 (2009) 3313–3321.
- [67] B. Volesky, J. Weber, J.M. Park, Continuous-flow metal biosorption in a regenerable Sargassum column, *Water Res.* 37 (2003) 297–306.
- [68] V. Padmavathy, Biosorption of nickel(II) ions by baker's yeast: Kinetic, thermodynamic and desorption studies, *Biore-source Technol.* 99 (2008) 3100–3109.
- [69] N.R. Shinde, A.V. Bankar, A.R. Kumar, S.S. Zinjarde, Removal of Ni (II) ions from aqueous solutions by biosorption onto two strains of *Yarrowia lipolytica*, *J. Environ. Manage.* 102 (2012) 115–124.
- [70] E. Malkoc, Ni(II) removal from aqueous solutions using cone biomass of *Thuja orientalis*, *J. Hazard. Mater.* 137 (2006) 899–908.
- [71] Z. Aksu, S. Ertuğrul, G. Donmez, Methylene Blue biosorption by *Rhizopus arrhizus*: Effect of SDS (sodium dodecylsulfate) surfactant on biosorption properties, *Chem. Eng. J.* 158 (2010) 474–481.
- [72] R. Abdallah, S. Taha, Biosorption of Methylene Blue from aqueous solution by nonviable *Aspergillus fumigatus*, *Chem. Eng. J.* 195–196 (2012) 69–76.
- [73] Y. Fu, T. Viraraghavan, Removal of Congo Red from an aqueous solution by fungus *Aspergillus niger*, *Adv. Environ. Res.* 7 (2002) 239–247.
- [74] B. Acemioglu, M. Kertmen, M. Digrak, M.H. Alma, Use of *Aspergillus wentii* for biosorption of Methylene Blue from aqueous solution, *Afr. J. Biotechnol.* 9(6) (2010) 874–881.
- [75] N. Das, Recovery of precious metals through biosorption—A review, *Hydrometallurgy* 103 (2010) 180–189.
- [76] L. Deng, Y. Su, H. Su, X. Wang, X. Zhu, Sorption and desorption of lead(II) from wastewater by green algae *Cladophora fascicularis*, *J. Hazard. Mater.* 143 (2007) 220–225.
- [77] M. Doğan, H. Abak, M. Alkan, Adsorption of Methylene Blue onto hazelnut shell: Kinetics, mechanism and activation parameters, *J. Hazard. Mater.* 164 (2009) 172–181.
- [78] J. German-Heins, M. Flury, Sorption of brilliant blue FCF in soils as affected by pH and ionic strength, *Geoderma* 97 (2000) 87–101.
- [79] Y. Guo, S. Yang, W. Fu, J. Qi, R. Li, Z. Wang, H. Xu, Adsorption of malachite green on micro and mesoporous rice husk-based active carbon, *Dyes Pigm.* 56 (2003) 219–229.
- [80] J.F. Gao, Q. Zhang, K. Su, J.H. Wang, Competitive biosorption of Yellow 2G and Reactive Brilliant Red K-2G onto inactive aerobic granules: Simultaneous determination of two dyes by first-order derivative spectrophotometry and isotherm studies, *Bioresour. Technol.* 101 (2010) 5793–5801.
- [81] S. Debnath, U.C. Ghosh, Equilibrium modeling of single and binary adsorption of Cd(II) and Cu(II) onto agglomerated nano structured titanium(IV) oxide, *Desalination* 273 (2011) 330–342.
- [82] Y. Goksungur, S. Uren, U. Guvenc, Biosorption of cadmium and lead ions by ethanol treated waste baker's yeast biomass, *Bioresour. Technol.* 96 (2005) 103–109.
- [83] Z. Aksu, G. Donmez, Binary biosorption of cadmium(II) and nickel(II) onto dried *Chlorella vulgaris*: Co-ion effect on mono-component isotherm parameters, *Process Biochem.* 41 (2006) 860–868.
- [84] G. Crini, P.M. Badot, Application of chitosan, a natural aminopolysaccharide, for dye removal from aqueous solutions by adsorption processes using batch studies: A review of recent literature, *Prog. Polym. Sci.* 33 (2008) 399–447.